

Dissipative spin chain as a non-Hermitian Kitaev ladder

Naoyuki Shibata* and Hosho Katsura
*Department of Physics, Graduate School of Science,
the University of Tokyo, Hongo, Tokyo 113-0033, Japan*
(Dated: May 4, 2022)

We derive exact results for the Lindblad equation for a quantum spin chain (one-dimensional quantum compass model) with dephasing noise. The system possesses doubly degenerate nonequilibrium steady states due to the presence of a conserved charge commuting with the Hamiltonian and Lindblad operators. We show that the system can be mapped to a non-Hermitian Kitaev model on a two-leg ladder, which is solvable by representing the spins in terms of Majorana fermions. This allows us to study the Liouvillian gap, the inverse of relaxation time, in detail. We find that the Liouvillian gap increases monotonically when the dissipation strength γ is small, while it decreases monotonically for large γ , implying a kind of phase transition in the first decay mode. The Liouvillian gap and the transition point are obtained in closed form in the case where the spin chain is critical. We also obtain the explicit expression for the autocorrelator of the edge spin. The result implies the suppression of decoherence when the spin chain is in the topological regime.

Introduction.—With recent advances in quantum engineering, it becomes increasingly important to study how the coupling to the environment affects a system. The time evolution of such an open system is described by a master equation. Under rather general conditions that the evolution is Markovian and Completely Positive and Trace Preserving (CPTP), one obtains the Lindblad equation [1] for the time-dependent density matrix. In the past, this quantum master equation had been mostly used to describe few-particle systems in, e.g., quantum optics. However, recent years have witnessed a growing interest in many-particle systems in the Lindblad setting [2–5].

Although there are several approaches to analyze the Lindblad equation such as perturbation theory [6, 7] and numerical methods [2, 8–10], exact results for the full dynamics is few and far between. In some cases [11, 12], the nonequilibrium steady states (NESSs) can be constructed exactly, but it is more challenging to completely diagonalize the Liouvillian (the generator of the Lindblad equation). In this sense, much fewer cases are known as exactly solvable models [5, 11]. The difficulty lies in dealing with the space of linear operators, the dimension of which grows more rapidly than that of the Hilbert space. This limits the system size amenable to exact numerical diagonalization. To make matters worse, it is often the case that effective interactions arise from dissipation even when the Hamiltonian itself is reducible to that of a free-particle system. This prevents us from understanding the full dynamics of the system.

In this Letter, we present an exactly solvable dissipative model which corresponds to the non-Hermitian many-body quantum system. The model we propose has a conserved charge that leads to two exact NESSs. Moreover, our model can be seen as a non-Hermitian Kitaev model on a two-leg ladder [13, 14]. Therefore, by applying Kitaev’s technique [15], our model can be mapped to

free Majorana fermions in a static \mathbb{Z}_2 gauge field, which allows us to fully diagonalize the Liouvillian. We numerically identify the gauge sectors where the first decay modes live. Then, assuming the flux configurations obtained, we derive the exact Liouvillian gap, the inverse of the relaxation time. We also study the infinite temperature autocorrelator of an edge spin and obtain its exact formula by applying techniques from combinatorics.

Models and NESSs.—We consider the Lindblad equation for the density matrix ρ

$$\frac{d\rho}{dt} = \mathcal{L}[\rho] := -i[H, \rho] + \sum_i \left(L_i \rho L_i^\dagger - \frac{1}{2} \{ L_i^\dagger L_i, \rho \} \right), \quad (1)$$

where H denotes the Hamiltonian of the one-dimensional quantum compass model [16–21] given by

$$H = - \sum_{i=1}^{N/2} J_x \sigma_{2i-1}^x \sigma_{2i}^x - \sum_{i=1}^{N/2-1} J_y \sigma_{2i}^y \sigma_{2i+1}^y, \quad (2)$$

and $L_i = \sqrt{\gamma} \sigma_i^z$ ($i = 1, \dots, N$) are Lindblad operators. Here σ_j^α ($\alpha = x, y, z$) are the Pauli operators at site j , and we assume that the number of sites N is even and the open boundary conditions are imposed. It suffices to consider the case $J_x, J_y \geq 0$, as the other cases can be obtained by an appropriate unitary transformation. The operator $\mathcal{L}[\rho]$ is called a Liouvillian or a Lindbladian. A NESS is a fixed point of the dynamics Eq. (1), i.e., an eigenstate of the Liouvillian \mathcal{L} with eigenvalue 0. For our model, there are two steady states $\rho_\pm := (\mathbb{1} \pm Q)/2^N$, where $\mathbb{1}$ is an identity matrix and $Q := \prod_i \sigma_i^z$ is a conserved charge, i.e.,

$$[H, Q] = 0, [L_i, Q] = [L_i^\dagger, Q] = 0 \quad \text{for } \forall i. \quad (3)$$

The proof goes as follows. Because of the Hermiticity of Lindblad operators, there is a trivial NESS, i.e., *completely mixed state* $\rho_c := \mathbb{1}/2^N$. One can easily verify

* shibata-naoyuki@g.ecc.u-tokyo.ac.jp

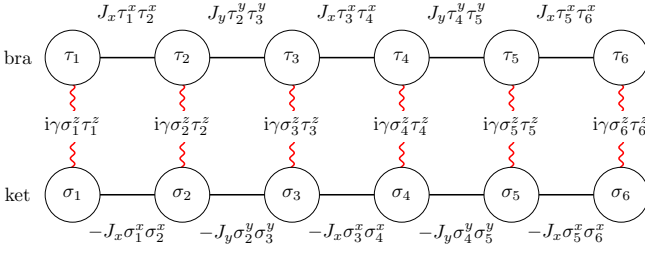


FIG. 1. The non-Hermitian ladder system for the one-dimensional quantum compass model with dephasing noise. By Kitaev’s mapping, this can be seen as a model of free Majorana fermions in a static \mathbb{Z}_2 gauge field. We fix all the signs of the links except for those of red wavy lines [22].

that if $\mathcal{L}[\rho_c] = 0$, then $\rho = Q\rho_c$ also satisfies $\mathcal{L}[\rho] = 0$. Although ρ itself is not positive semi-definite which is a necessary condition to be a density operator, one can construct the following operators $P_{\pm} := (1 \pm Q)/2$, which are orthogonal projections, and hence positive semi-definite. This then gives (normalized) steady states $\rho_{\pm} = P_{\pm}/\text{tr} P_{\pm}$. We have checked numerically for small N that they are the unique NESS of the system.

Kitaev’s Mapping.—A $2^N \times 2^N$ density matrix ρ can be thought of as a 2^{2N} -dimensional vector (See Supplemental Material [22] for details). In this sense, we can identify the Liouvillian \mathcal{L} for the one-dimensional chain as a non-Hermitian Hamiltonian of a ladder system [3, 4] (see Fig. 1):

$$i(\mathcal{L} + \gamma N) \cong H \otimes \mathbb{1} - \mathbb{1} \otimes H + \sum_{i=1}^N i\gamma \sigma_i^z \otimes \tau_i^z =: \mathcal{H}, \quad (4)$$

where the Hilbert space of the RHS is the “Ket \otimes Bra space” and τ_i^z is the Pauli matrix for the i th Bra site. The non-unitary terms in the Liouvillian (1) correspond to the non-Hermitian terms in \mathcal{H} .

We apply to this ladder Hamiltonian (4) the technique by Kitaev [15], which was originally used to solve the quantum spin model on a honeycomb lattice. In order to solve the model, Kitaev developed an elegant technique: substituting *Majorana fermion operators* for spin operators $\sigma_j^{\alpha} \rightarrow ib_j^{\alpha} c_j$. Here, b_j^{α} and c_j are Majorana operators obeying the Clifford algebra $\{c_j, c_k\} = 2\delta_{jk}$, $\{b_j^{\alpha}, b_k^{\beta}\} = 2\delta_{jk}\delta^{\alpha\beta}$, and $\{b_j^{\alpha}, c_k\} = 0$ with $\{A, B\} = AB + BA$ being the anti-commutator. After the mapping, we have a quadratic Hamiltonian of itinerant Majorana fermions (c_i ’s) in each sector specified by the static \mathbb{Z}_2 gauge field (i.e., each link has the sign ± 1 in the hopping amplitude). Thus, we can diagonalize the Hamiltonian and obtain all eigenvalues and eigenstates, sector by sector. Besides the honeycomb lattice, Kitaev’s mapping is applicable to other lattices with a similar Hamiltonian. Examples include the ladder system [13], which is the Hermitian analogue of our model (4).

Next, we define usual Dirac fermions f_i, f_i^{\dagger} each of which is made of two Majorana fermions c_i and d_i :

$f_i := (c_i + id_i)/2$, $f_i^{\dagger} := (c_i - id_i)/2$. Here, c_i (resp. d_i) is the Majorana operator for the σ_i (resp. τ_i) spin. Then, the model is mapped to the Su-Schrieffer-Heeger (SSH) model [23] with imaginary chemical potential [24, 25]. The Hamiltonian reads [22]

$$\mathcal{H}(\boldsymbol{\mu}) = -\sum_{i=1}^N i\gamma \mu_i + \sum_{k,l} A_{kl} f_k^{\dagger} f_l, \quad (5)$$

where $\boldsymbol{\mu} = (\mu_1, \dots, \mu_N)$ and A is a tridiagonal and complex-symmetric matrix given by

$$A := 2 \begin{pmatrix} i\gamma \mu_1 & J_x & & & & \\ J_x & i\gamma \mu_2 & J_y & & & \\ & J_y & i\gamma \mu_3 & \ddots & & \\ & & \ddots & \ddots & J_x & \\ & & & & J_x & i\gamma \mu_N \end{pmatrix}. \quad (6)$$

μ_i ’s come from the gauge degree of freedom and take the value ± 1 . The solution of a non-Hermitian quadratic form of fermions is similar to that of a Hermitian one. One can construct many-body eigenstates of $\mathcal{H}(\boldsymbol{\mu})$ by just filling single-particle energies of the Hamiltonian, which can be obtained by diagonalizing A .

Symmetries of the Hamiltonian (5) enable us to restrict the configurations of μ_i ’s to consider. First, $\mathcal{H}(\boldsymbol{\mu})$ and $\mathcal{H}(-\boldsymbol{\mu})$ have the same spectrum because the flux configuration in the ladder system is invariant under sending $\boldsymbol{\mu} \rightarrow -\boldsymbol{\mu}$. (In view of the SSH model, $\mathcal{H}(\boldsymbol{\mu})$ is transformed to $\mathcal{H}(-\boldsymbol{\mu})$ by the charge conjugation $f_j \rightarrow (-1)^j f_j^{\dagger}$.) Second, due to the inversion symmetry, the transformation $(\mu_1, \mu_2, \dots, \mu_N) \rightarrow (\mu_N, \mu_{N-1}, \dots, \mu_1)$ leaves the spectrum of \mathcal{H} unchanged. In the following, we only consider the configurations in which the number of positive μ_i ’s is not less than the number of negative μ_i ’s.

Liouvillian gap.—Let eigenvalues of the Liouvillian \mathcal{L} be $\Lambda_i(\mathcal{L})$. It can be proved [1, 26] that all $\Lambda_i(\mathcal{L})$ satisfy $\text{Re}[\Lambda_i(\mathcal{L})] \leq 0$. A Liouvillian gap g is defined as

$$g := -\max_{\text{Re}[\Lambda_i(\mathcal{L})] \neq 0} \text{Re}[\Lambda_i(\mathcal{L})], \quad (7)$$

hence, the inverse of the relaxation time. It is clear from Eqs. (4) and (7) that the Liouvillian gap corresponds to the gap between the first and second largest *imaginary* parts of eigenvalues of \mathcal{H} , the former of which is γN . The configuration which gives the eigenvalue $i\gamma N$ is $\mu_i = +1$ for all i . The reason is as follows. In this configuration, the one-particle energy levels are obtained just by shifting those of the original SSH model by $+2i\gamma$. Therefore, we obtain the eigenvalue $i\gamma N$ by filling all the energy levels.

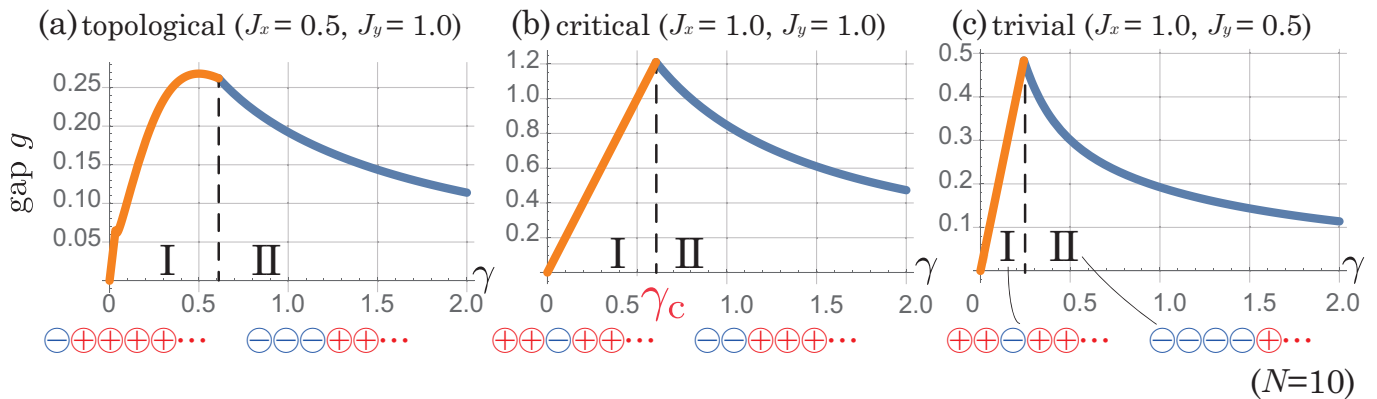


FIG. 2. (Color online) Numerical results of the Liouvillian gap g as a function of the dissipation strength γ . (a) Topological regime ($J_x = 0.5$, $J_y = 1.0$), (b) critical point ($J_x = J_y = 1.0$), and (c) trivial regime ($J_x = 1.0$, $J_y = 0.5$). The position of the cusp is indicated by the dashed line in each case. The $+/-$ pattern below each phase shows a chemical-potential configuration μ that gives the first decay mode.

Then, the Liouvillian gap is recast as

$$g = \gamma N - \max_{\mu, m(\mu) \neq 0} \left[\sum_{i=1}^N \left(\frac{\text{Im } \lambda_i + |\text{Im } \lambda_i|}{2} - \gamma \mu_i \right) \right]$$

$$= \min_{\mu, m(\mu) \neq 0} \left(2m(\mu)\gamma - \sum_{i=1}^N \frac{|\text{Im } \lambda_i| - \text{Im } \lambda_i}{2} \right), \quad (8)$$

where λ_i denotes the i th eigenvalue of A , and $m(\mu)$ the number of μ_i 's which are -1 . Since at least one of μ_i 's must be -1 when $m(\mu) \neq 0$, we have $g \leq 2\gamma$. One might think that we need to consider the case where $\mu_i = +1$ for all i and some single-particle energy levels are empty. However, this is not the case. The Liouvillian gap in this sector must be greater than or equal to g in Eq. (8), as removing one fermion from an occupied state in this case decreases the imaginary part of the eigenvalue of \mathcal{H} by 2γ . Thus, it suffices to consider configurations different from the one with $\mu_i = +1$ for all i .

Fig. 2 shows the numerical results of g as a function of γ for various J_y/J_x for a system size $N = 10$. Here, ‘topological’, ‘critical’, and ‘trivial’ cases refer to the regions $J_y/J_x > 1$, $J_y = J_x$, and $J_y/J_x < 1$, respectively, in analogy with the Hermitian SSH model. From this figure, we can see a kind of phase transition of the first decay mode in every (topological, critical, or trivial) case. We also numerically obtained the chemical-potential configurations which give the first decay mode, as also shown in Fig. 2 [27]. In the ‘phase I’ of the critical and topological cases, the gap behaves as exactly $g = 2\gamma$. The reason for this behavior becomes clear in Eq. (8). When γ is small enough, all λ_i satisfy $\text{Im } \lambda_i > 0$, then $g = 2\gamma$ follows. In the topological case, the situation is slightly different. In this case there exists a λ_i which satisfies $\text{Im } \lambda_i < 0$, and g is smaller than 2γ . For finite N , there is another configuration in the region of $\gamma \ll 1$ [22], but this region shrinks to zero as $N \rightarrow \infty$. In the ‘phase II’, the gap behaves asymptotically $g \propto 1/\gamma$ in each case. This increase

in relaxation time as $\gamma \rightarrow \infty$ can be thought of as the Quantum Zeno effect [28].

Our extensive numerical calculation suggests that the chemical-potential configurations which give the first decay modes do not depend on the system size. Then, under this assumption, we can obtain the exact formula for the Liouvillian gap g and the transition point γ_c in the thermodynamic limit of the critical case $J_x = J_y = 1$ (see [22] for more details):

$$g = \begin{cases} 2\gamma & (0 \leq \gamma \leq \gamma_c) \\ \frac{6^{1/3} \left(9\gamma^2 + \sqrt{48\gamma^6 + 81\gamma^4} \right)^{2/3} - 2 \cdot 6^{2/3} \gamma^2}{3\gamma \left(9\gamma^2 + \sqrt{48\gamma^6 + 81\gamma^4} \right)^{1/3}} & (\gamma_c \leq \gamma) \end{cases}, \quad (9)$$

where

$$\gamma_c = \sqrt{\frac{\sqrt{3}-1}{2}} \simeq 0.605. \quad (10)$$

We have confirmed that this result agrees well with the numerical one for $N = 10$.

Autocorrelator at $T = \infty$.—In this section, we study the ‘infinite temperature’ autocorrelator of the edge spin

$$C_\infty(t) := \langle \sigma_1^z(t) \sigma_1^z(0) \rangle_{T=\infty} = \frac{1}{2^N} \text{tr} \left(e^{t\mathcal{L}^*} [\sigma_1^z] \sigma_1^z \right), \quad (11)$$

where \mathcal{L}^* is the adjoint operator of the Liouvillian, which describes the time evolution of an operator X as follows:

$$\frac{d}{dt} X(t) = \mathcal{L}^*[X(t)]$$

$$:= i[H, X(t)] + \sum_i \left(L_i^\dagger X(t) L_i - \frac{1}{2} \{ L_i^\dagger L_i, X(t) \} \right). \quad (12)$$

In other words, it corresponds to the Heisenberg picture of the open quantum system. A fundamental motivation

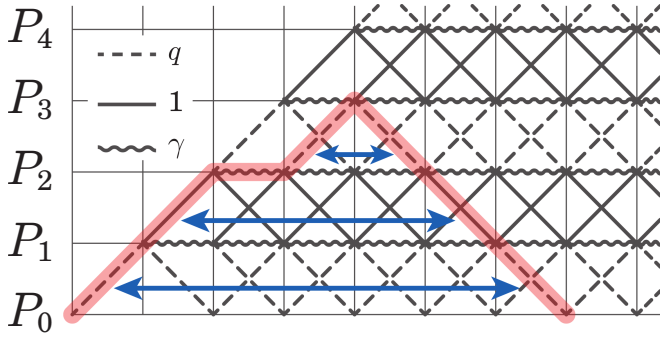


FIG. 3. An example of the weighted Riordan paths. Each path is from $(0,0)$ to $(n,0)$ with up (\nearrow), down (\searrow), and horizontal (\rightarrow) steps, never going below the bottom line nor containing horizontal steps on it. Dashed (wavy horizontal) steps are endowed with a weight q (r), which yields the weight of each Riordan path. For instance, the red path from $(0,0)$ to $(7,0)$ has a weight $q^4\gamma$. The sign of a weight is plus (resp. minus) if $(\# \text{ of matched up-down pairs depicted by blue double-headed arrows}) + (\# \text{ of horizontal steps})$ is even (resp. odd).

in quantum engineering is for localized degrees of freedom to maintain coherence over long times. In [29], this quantity for the transverse-field Ising and XYZ chains without dissipation (i.e., closed system) has been studied as the witness of long coherence times for edge spins. The autocorrelator for the dissipative transverse-field Ising model was also studied in [28]. Here, we study $C_\infty(t)$ for our model with $N = \infty$. Let us consider how the adjoint Liouvillian acts on σ_1^z . For notational simplicity, we set $J_x = q/2$, $J_y = 1/2$ and $r := \gamma/4$. In this case, one finds

$$\mathcal{L}^*[P_0] = qP_1, \quad (13)$$

and for $n \geq 1$,

$$\mathcal{L}^*[P_n] = \begin{cases} -qP_{n-1} - rP_n - P_{n+1} & (n: \text{ odd}) \\ P_{n-1} - rP_n + qP_{n+1} & (n: \text{ even}) \end{cases} \quad (14)$$

where

$$P_0 = \sigma_1^z, \quad P_n = \begin{cases} -\sigma_1^y \left(\prod_{i=2}^n \sigma_i^z \right) \sigma_{n+1}^x & (n: \text{ odd}) \\ -\sigma_1^y \left(\prod_{i=2}^n \sigma_i^z \right) \sigma_{n+1}^y & (n \geq 2 \text{ and even}) \end{cases}. \quad (15)$$

It is important to note that P_n 's are Hermitian and form an orthonormal set, i.e.,

$$\langle\langle P_i, P_j \rangle\rangle := \frac{1}{2^N} \text{tr} \left(P_i^\dagger P_j \right) = \delta_{ij}.$$

The inner product $\langle\langle \cdot, \cdot \rangle\rangle$ for matrices is called the Hilbert-Schmidt inner product, with which Eq. (11) takes the

form

$$C_\infty(t) = \sum_{n=0}^{\infty} \frac{t^n}{n!} \langle\langle \mathcal{L}^{*n}[P_0], P_0 \rangle\rangle. \quad (16)$$

Now we compute $C_\infty(t)$ by considering the so called ‘Riordan paths’ [30, 31] (Motzkin paths [32] with no horizontal steps at the bottom line) weighted through q and r . (see Fig. 3). To this end, it is useful to consider the generating function $F(z; q, r)$ of the weighted Riordan paths, which can be obtained by the so called ‘Kernel method’ [33]. The autocorrelator in terms of $F(z; q, r)$ reads

$$C_\infty(t) = \sum_{n=0}^{\infty} \frac{t^n}{n!} [z^n] F(z; q, r) \quad (17)$$

where $[z^n]f(z)$ denotes the coefficient of z^n in $f(z)$. This can be rewritten as a contour integral

$$C_\infty(t) = \sum_{n=0}^{\infty} \frac{t^n}{n!} \oint \frac{dz}{2\pi i} \frac{F(z; q, r)}{z^{n+1}} \quad (18)$$

$$= \frac{1}{2\pi i} \oint \frac{F(1/w; q, r)}{w} e^{tw} dw, \quad (19)$$

where $w = 1/z$. Here we have chosen the contour in the z -plane so that it surrounds the origin and is sufficiently small. As a result, the contour in the w -plane is sufficiently large. The final explicit expression for $C_\infty(t)$ is cumbersome and is not shown here [22]. But from the result, we can derive the inverse of the decay time τ of the autocorrelator: for $0 < q < 1$, one has

$$\tau^{-1} = -\eta_+(q, r), \quad (20)$$

and for $q > 1$,

$$\tau^{-1} = \begin{cases} r & (0 < r < 1) \\ \frac{1+r^2}{2r} & (1 < r < q + \sqrt{q^2 - 1}) \\ -\eta_+(q, r) & (r > q + \sqrt{q^2 - 1}) \end{cases}, \quad (21)$$

where $\eta_+(q, r) := (-1 - r^2 + \sqrt{(1+r^2)^2 - 4q^2r^2})/(2r)$. In particular, we find that the decay is suppressed in the topological regime ($0 < q < 1$), although $C_\infty(t)$ goes to 0 as $t \rightarrow \infty$ in both regime.

Conclusions.—We have studied the one-dimensional quantum compass model with dephasing noise and obtained the exact steady states. We showed that the model can be mapped to the non-Hermitian Kitaev model on a ladder, which is solvable by representing the spins in terms of Majorana fermions. This technique allows us to study the Liouvillian gap exactly. In particular, in the critical case where $J_x = J_y$, the gap in the thermodynamic limit is obtained analytically. We have also studied the autocorrelator of the edge spin and obtained its exact formula using the technique of combinatorics.

Acknowledgments.—We would like to thank T. Prosen and M. Žnidarič for valuable comments. H.K. was supported in part by JSPS KAKENHI Grant Nos. JP18H04478 and JP18K03445. N.S. acknowledges support of the Materials Education program for the future leaders in Research, Industry, and Technology (MERIT).

-
- [1] H.-P. Breuer and F. Petruccione, *The Theory of Open Quantum Systems* (Oxford University Press, 2002).
- [2] T. Prosen and M. Žnidarič, *J. Stat. Mech.* (2009) P02035.
- [3] M. Žnidarič, *Phys. Rev. E* **89**, 042140 (2014).
- [4] M. Žnidarič, *Phys. Rev. E* **92**, 042143 (2015).
- [5] M. V. Medvedyeva, F. H. L. Essler, and T. Prosen, *Phys. Rev. Lett.* **117**, 137202 (2016).
- [6] M. R. Gallis, *Phys. Rev. A* **53**, 655 (1996).
- [7] A. C. Y. Li, F. Petruccione, and J. Koch, *Sci. Rep.* **4**, 4887 (2014).
- [8] J. Cui, J. I. Cirac, and M. C. Bañuls, *Phys. Rev. Lett.* **114**, 220601 (2015).
- [9] A. Kshetrimayum, H. Weimer, and R. n Orús, *Nat. Comm.* **8**, 1291 (2017).
- [10] M. Raghunandan, J. Wrachtrup, and H. Weimer, *Phys. Rev. Lett.* **120**, 150501 (2018).
- [11] T. Prosen, *New J. Phys.* **10**, 043026 (2008).
- [12] T. Prosen, *Phys. Rev. Lett.* **107**, 137201 (2011).
- [13] W. DeGottardi, D. Sen, and S. Vishveshwara, *New J. Phys.* **13**, 065028 (2011).
- [14] N. Wu, *Phys. Lett. A* **376**, 3530 (2012).
- [15] A. Kitaev, *Ann. Phys.* **321**, 2 (2006).
- [16] W. Brzezicki, J. Dziarmaga, and A. M. Oleś, *Phys. Rev. B* **75**, 134415 (2007).
- [17] X.-Y. Feng, G.-M. Zhang, and T. Xiang, *Phys. Rev. Lett.* **98**, 087204 (2007).
- [18] W.-L. You and G.-S. Tian, *Phys. Rev. B* **78**, 184406 (2008).
- [19] E. Eriksson and H. Johannesson, *Phys. Rev. B* **79**, 224424 (2009).
- [20] R. Jafari, *Phys. Rev. B* **84**, 035112 (2011).
- [21] G.-H. Liu, W. Li, W.-L. You, G.-S. Tian, and G. Su, *Phys. Rev. B* **85**, 184422 (2012).
- [22] See Supplemental Material for details.
- [23] W. P. Su, J. R. Schrieffer, and A. J. Heeger, *Phys. Rev. Lett.* **42**, 1698 (1979).
- [24] M. Klett, H. Cartarius, D. Dast, J. Main, and G. Wunner, *Phys. Rev. A* **95**, 053626 (2017).
- [25] S. Lieu, *Phys. Rev. B* **97**, 045106 (2018).
- [26] Ángel Rivas and S. F. Huelga, *Open Quantum Systems: An Introduction* (SpringerBriefs in Physics, 2011).
- [27] We do not show all the configurations which give the same eigenvalues. In [22], up to symmetries mentioned above, every configuration which gives the first decay mode is shown.
- [28] L. M. Vasiloiu, F. Carollo, and J. P. Garrahan, *Phys. Rev. B* **98**, 094308 (2018).
- [29] J. Kemp, N. Y. Yao, C. R. Laumann, and P. Fendley, *J. Stat. Mech.* (2017), 063105.
- [30] W. Y. Chen, E. Y. Deng, and L. L. Yang, *Discrete Math.* **308**, 2222 (2008).
- [31] E. Cohen, T. Hansen, and N. Itzhaki, *Sci. Rep.* **6**, 30232 (2016).
- [32] R. P. Stanley, *Enumerative Combinatorics vol. 2* (Cambridge University Press, 1999).
- [33] H. Prodinger, *Sém. Lothar. Combin.* **50**, Art. B50f, 19 pp. (electronic) (2003/04).
- [34] D. C. Brody, *J. Phys. A: Math. Theor.* **47**, 035305 (2014).
- [35] M. M. Sternheim and J. F. Walker, *Phys. Rev. C* **6**, 114 (1972).
- [36] W. D. Heiss, *J. Phys. A: Math. Theor.* **45**, 444016 (2012).
- [37] U. Bilstein and B. Wehefritz, *J. Phys. A: Math. Gen.* **32**, 191 (1998).

Supplemental Materials for: Dissipative spin chain as a non-Hermitian Kitaev ladder

I. MAPPING OF THE LIOUVILLIAN TO THE NON-HERMITIAN HAMILTONIAN

In this section, we explain more details on identifying the Liouvillian as a non-Hermitian Hamiltonian. Let A be a linear operator on Hilbert space \mathcal{H} (i.e., $A \in \text{End}_{\mathbb{C}}(\mathcal{H})$). Assuming $\dim(\mathcal{H}) = N$, there is a complete orthonormal basis $\{|\phi_i\rangle\}_{i=1}^N$ of \mathcal{H} , and A can be regarded as an $N \times N$ matrix

$$A = \sum_{i,j=1}^N A_{ij} |\phi_i\rangle \langle \phi_j|, \quad (22)$$

where a sans-serif style $A \in M_{N \times N}(\mathbb{C})$ and its element A_{ij} is just a c-number. Now, we introduce a new space $\text{Ket} \otimes \text{Bra}$ of dimension N^2 by the following linear map F :

$$\begin{array}{ccc} F : \text{End}_{\mathbb{C}}(\mathcal{H}) & \longrightarrow & \text{Ket} \otimes \text{Bra} \\ \Downarrow & & \Downarrow \\ & & |\phi_i\rangle \langle \phi_j| \longmapsto |\phi_i, \phi_j\rangle \end{array} \quad (23)$$

Note that F depends on the choice of the basis $\{|\phi_i\rangle\}_{i=1}^N$, but after fixing the basis, F is an isomorphism, i.e., $\text{End}_{\mathbb{C}}(\mathcal{H})$ and $\text{Ket} \otimes \text{Bra}$ are in one-to-one correspondence.

Let us consider how superoperators ($\in \text{End}_{\mathbb{C}}(\text{End}_{\mathbb{C}}(\mathcal{H}))$) look like in the $\text{Ket} \otimes \text{Bra}$ space. All superoperators in the Lindbladian $\mathcal{L}[\rho]$ have the form

$$\rho \mapsto A\rho B. \quad (24)$$

This map is rewritten in the language of matrices as

$$\sum_{i,j} R_{ij} |\phi_i\rangle \langle \phi_j| \mapsto \sum_{i,j} (\text{ARB})_{ij} |\phi_i\rangle \langle \phi_j| \quad (25)$$

for $A = \sum_{i,j} A_{ij} |\phi_i\rangle \langle \phi_j|$, $B = \sum_{i,j} B_{ij} |\phi_i\rangle \langle \phi_j|$ and $\rho = \sum_{i,j} R_{ij} |\phi_i\rangle \langle \phi_j|$. In the Ket \otimes Bra space, the superoperator is seen as the following map:

$$\begin{aligned} \sum_{i,j} R_{ij} |\phi_i, \phi_j\rangle\rangle &\mapsto \sum_{i,j} (\text{ARB})_{ij} |\phi_i, \phi_j\rangle\rangle \\ &= \left[\left(\sum_{i,k} A_{ik} |\phi_i\rangle\rangle \langle\langle \phi_k| \right)_{\text{Ket}} \otimes \left(\sum_{j,l} B_{jl}^T |\phi_j\rangle\rangle \langle\langle \phi_l| \right)_{\text{Bra}} \right] \sum_{m,n} R_{mn} |\phi_m, \phi_n\rangle\rangle. \end{aligned} \quad (26)$$

Therefore, this superoperator $\rho \mapsto A\rho B$ can be thought of as the tensor product of two matrix $A \otimes B^T$. (Note that this matrix is basis-dependent because it is not $A \otimes B^\dagger$.) Then, one can identify the Liouvillian \mathcal{L} in Eq. (1) as

$$\begin{aligned} \mathcal{L} &\cong -iH \otimes \mathbb{1} + i\mathbb{1} \otimes H^T \\ &+ \sum_i \left(L_i \otimes L_i^* - \frac{1}{2} L_i^\dagger L_i \otimes \mathbb{1} - \frac{1}{2} \mathbb{1} \otimes L_i^T L_i^* \right). \end{aligned} \quad (27)$$

(Here, we do not distinguish operators in italic font with matrices in sans-serif font.) For Eq. (4), transpose or conjugate in Eq. (27) does not matter if we choose a basis which diagonalizes σ_i^z 's.

II. NON-HERMITIAN QUADRATIC FORM OF FERMIONS

In a usual closed free fermionic system, we can generally write the Hamiltonian as follows:

$$H = \mathbf{f}^\dagger \mathbf{A} \mathbf{f}, \quad (28)$$

where $\mathbf{f} = (f_1, \dots, f_N)^T$, $\mathbf{f}^\dagger = (f_1^\dagger, \dots, f_N^\dagger)$, and \mathbf{A} is an $N \times N$ Hermitian matrix. In general, all eigenvalues of a Hermitian matrix are real, and eigenvectors can form an orthonormal basis (after normalization and orthogonalization in degenerate spaces). In other words, \mathbf{A} can be diagonalized by a unitary matrix \mathbf{U} , and the Hamiltonian is rewritten as

$$H = \mathbf{f}^\dagger \mathbf{U} \text{diag}(a_1, \dots, a_N) \mathbf{U}^\dagger \mathbf{f}, \quad (29)$$

where a_i ($i = 1, \dots, N$) are the eigenvalues of \mathbf{A} . Then, we can define new operators $\mathbf{f}' := \mathbf{U}^\dagger \mathbf{f}$, and it is easily verified that \mathbf{f}' also satisfy anticommutation relations. Therefore, we obtain

$$H = \sum_{i=1}^N a_i f_i'^\dagger f_i', \quad (30)$$

and all eigenvalues of H are obtained by $E = \sum_i a_i n_i$ with arbitrary choice of each $n_i = 0$ or 1.

However, some care must be taken when \mathbf{A} is non-Hermitian. First, eigenvalues of \mathbf{A} are not necessarily real. Second, eigenvectors with different eigenvalues are in general not orthogonal. Third, left and right eigenvectors with the same eigenvalue are in general not a Hermitian-conjugate to each other. We briefly explain the general prescription for treating non-Hermitian matrices according to Ref. [34]. A similar discussion can be found in Ref. [35].

Let \mathbf{A} be a non-Hermitian and non-degenerate $N \times N$ matrix. Remember that if a matrix is non-degenerate, then it is diagonalizable. We can easily generalize the following discussion to the case where \mathbf{A} is degenerate but diagonalizable. However, some degenerate matrices cannot be diagonalized, and such situations are sometimes called ‘‘coalescence’’ instead of ‘‘degeneracy’’. We do not consider ‘‘coalescence’’ here. See, e.g., Ref. [36] for more details about coalescence. Then, \mathbf{A} has left/right eigenvectors $\{\mathbf{l}_i^\dagger\}_{i=1}^N$ and $\{\mathbf{r}_j\}_{j=1}^N$ which satisfy

$$\mathbf{l}_i^\dagger \mathbf{A} = \lambda_i \mathbf{l}_i^\dagger \quad (31)$$

$$\mathbf{A} \mathbf{r}_j = \xi_j \mathbf{r}_j. \quad (32)$$

(\mathbf{l}_i and \mathbf{r}_j are column vectors.) From these, we obtain

$$\begin{aligned}\lambda_i \langle \mathbf{l}_i, \mathbf{r}_j \rangle &= \mathbf{l}_i^\dagger \mathbf{A} \mathbf{r}_j = \xi_j \langle \mathbf{l}_i, \mathbf{r}_j \rangle \\ \therefore (\lambda_i - \xi_j) \langle \mathbf{l}_i, \mathbf{r}_j \rangle &= 0,\end{aligned}\tag{33}$$

where $\langle \mathbf{l}_i, \mathbf{r}_j \rangle := \mathbf{l}_i^\dagger \mathbf{r}_j$ is the standard inner product of \mathbb{C}^N . Because \mathbf{A} is diagonalizable, each of $\{\mathbf{l}_i\}_{i=1}^N$ and $\{\mathbf{r}_j\}_{j=1}^N$ is a basis of \mathbb{C}^N . Therefore, fixing index i and making index j run, at least one j satisfies $\langle \mathbf{l}_i, \mathbf{r}_j \rangle \neq 0$. Then, we can assume $\lambda_i = \xi_i$ after relabeling j 's. It follows that $\langle \mathbf{l}_i, \mathbf{r}_j \rangle = 0$ if $i \neq j$ and $\langle \mathbf{l}_i, \mathbf{r}_i \rangle \neq 0$. Therefore, after ‘‘normalization’’ of $\{\mathbf{l}_i\}_{i=1}^N$ and/or $\{\mathbf{r}_j\}_{j=1}^N$ so as to satisfy $\langle \mathbf{l}_i, \mathbf{r}_i \rangle = 1$, we obtain

$$\langle \mathbf{l}_i, \mathbf{r}_j \rangle = \delta_{ij}.\tag{34}$$

Then, we define

$$\mathbf{V} := (\mathbf{r}_1 \dots \mathbf{r}_N) \left(\iff \mathbf{V}^{-1} = \begin{pmatrix} \mathbf{l}_1^\dagger \\ \vdots \\ \mathbf{l}_N^\dagger \end{pmatrix} \right),\tag{35}$$

and \mathbf{A} is diagonalized as

$$\mathbf{V}^{-1} \mathbf{A} \mathbf{V} = \text{diag}(\lambda_1, \dots, \lambda_N).\tag{36}$$

Now, let us return to Eq. (28) with non-Hermitian \mathbf{A} . By diagonalizing \mathbf{A} as above, we obtain

$$\mathbf{H} = \mathbf{f}^\dagger \mathbf{V} \text{diag}(\lambda_1, \dots, \lambda_N) \mathbf{V}^{-1} \mathbf{f}\tag{37}$$

and we define

$$a_i := \mathbf{l}_i^\dagger \mathbf{f}, \quad b_i^\dagger := \mathbf{f}^\dagger \mathbf{r}_i,\tag{38}$$

then, the Hamiltonian can be written in the form similar to Eq. (30),

$$\mathbf{H} = \sum_{i=1}^N \lambda_i b_i^\dagger a_i.\tag{39}$$

One can easily verify the following anticommutation relations

$$\{a_i, b_j^\dagger\} = \delta_{ij}, \quad \{a_i, a_j\} = \{b_i^\dagger, b_j^\dagger\} = 0.\tag{40}$$

Therefore, a_i and b_i^\dagger can be seen as an annihilation and an creation operator of new fermions respectively, although a_i^\dagger is not equal to b_i^\dagger unlike Hermitian cases [37]. From these anticommutation relations, it follows that $b_i^\dagger a_i$ has eigenvalues 0 and 1, although it is not Hermitian. Then we obtain all eigenvalues of \mathbf{H} as $E = \sum_i \lambda_i n_i$ with arbitrary choice of each $n_i = 0$ or 1.

III. FROM KITAEV LADDER TO SSH MODEL

By Kitaev’s mapping, a non-Hermitian Hamiltonian \mathcal{H} can be seen as a model of free Majorana fermions in a static \mathbb{Z}_2 gauge field. Introducing Majorana fermion operators as $\sigma_j^\alpha \rightarrow i b_j^\alpha c_j$ and $\tau_j^\alpha \rightarrow i \tilde{b}_j^\alpha d_j$ ($i = 1, \dots, N$, $\alpha = x, y, z$), we obtain

$$\begin{aligned}\mathcal{H} &= J_x \sum_{j=1}^{N/2} \left[(i b_{2j-1}^x b_{2j}^x) (i c_{2j-1} c_{2j}) - (i \tilde{b}_{2j-1}^x \tilde{b}_{2j}^x) (i d_{2j-1} d_{2j}) \right] + J_y \sum_{j=1}^{N/2-1} \left[(i b_{2j}^y b_{2j+1}^y) (i c_{2j} c_{2j+1}) - (i \tilde{b}_{2j}^y \tilde{b}_{2j+1}^y) (i d_{2j} d_{2j+1}) \right] \\ &\quad - i\gamma \sum_{i=1}^N (i b_i^z \tilde{b}_i^z) (i c_i d_i),\end{aligned}\tag{41}$$

where the operators, $ib_{2j-1}^x b_{2j}^x$, $ib_{2j}^y b_{2j+1}^y$, $i\tilde{b}_{2j-1}^x \tilde{b}_{2j}^x$, $i\tilde{b}_{2j}^y \tilde{b}_{2j+1}^y$, and $ib_i^z \tilde{b}_i^z$ commute with the Hamiltonian and their eigenvalues are ± 1 . Therefore, the Hilbert space splits into sectors labeled by the eigenvalue of the product of b and \tilde{b} operators around it. One can define the flux through each plaquette by the eigenvalue of the product of b and \tilde{b} operators around it. The spectrum of the Hamiltonian \mathcal{H} depends only on the set of fluxes. Thus, we can fix all but $N - 1$ signs of the links, as we have $N - 1$ plaquettes in our model. We fix them as

$$ib_{2j-1}^x b_{2j}^x = ib_{2j}^y b_{2j+1}^y = -1, \quad i\tilde{b}_{2j-1}^x \tilde{b}_{2j}^x = i\tilde{b}_{2j}^y \tilde{b}_{2j+1}^y = +1 \quad (42)$$

and define $\mu_i = -ib_i^z \tilde{b}_i^z$ to recast \mathcal{H} as

$$\mathcal{H} = -J_x \sum_{j=1}^{N/2} [(ic_{2j-1} c_{2j}) + (id_{2j-1} d_{2j})] - J_y \sum_{j=1}^{N/2-1} [(ic_{2j} c_{2j+1}) + (id_{2j} d_{2j+1})] + i\gamma \sum_{i=1}^N \mu_i (ic_i d_i). \quad (43)$$

Next, we define usual Dirac fermions f_i and f_i^\dagger , consisting of two Majorana fermions c_i and d_i :

$$f_i := \frac{c_i + id_i}{2}, \quad f_i^\dagger := \frac{c_i - id_i}{2}. \quad (44)$$

It is easy to verify that they satisfy the anti-commutation relations

$$\{f_i, f_j^\dagger\} = \delta_{ij}, \quad \{f_i, f_j\} = \{f_i^\dagger, f_j^\dagger\} = 0. \quad (45)$$

We then have

$$\mathcal{H} = 2iJ_x \sum_{i=1}^{N/2} (f_{2j}^\dagger f_{2j-1} - f_{2j-1}^\dagger f_{2j}) + 2iJ_y \sum_{i=1}^{N/2-1} (f_{2j+1}^\dagger f_{2j} - f_{2j}^\dagger f_{2j+1}) + i\gamma \sum_{i=1}^N \mu_i (2f_i^\dagger f_i - 1). \quad (46)$$

After the unitary transformation $f_j \rightarrow e^{i(\pi/2)j} f_j$, we obtain Eq. (5).

IV. THE FIRST DECAY MODES' CONFIGURATIONS

In Fig. 2, we show for each phase only one example of the configurations where the first decay mode lives, but numerical calculation reveals that there are other such configurations. Tab. I shows the numerical results of all such configurations up to symmetries mentioned in the main text.

TABLE I.

| | very small- γ phase | phase I | phase II |
|-------------|--|---|--|
| topological | $\begin{cases} \mu_i = -1 & i = 1, N \\ \mu_i = +1 & \text{otherwise} \end{cases}$ | $\begin{cases} \mu_i = -1 & i = 1 \\ \mu_i = +1 & \text{otherwise} \end{cases}$ | $\begin{cases} \mu_i = -1 & i = 1, 2, 3 \\ \mu_i = +1 & \text{otherwise} \end{cases}$ |
| critical | $\exists! i \text{ s.t. } \mu_i = -1, \text{ and } \mu_j = +1 \text{ for } j \neq i$ | | $\begin{cases} \mu_i = -1 & i = 1, 2 \\ \mu_i = +1 & \text{otherwise} \end{cases}$ |
| trivial | $\exists! i \text{ s.t. } \mu_i = -1, \text{ and } \mu_j = +1 \text{ for } j \neq i$ | | $\begin{cases} \mu_i = -1 & i = 1, 2, 3, 4 \\ \mu_i = +1 & \text{otherwise} \end{cases}$ |

V. DERIVATION OF EQ. (9)

We call the pattern of $\boldsymbol{\mu}$ which satisfies “ $\mu_1 = -1$, otherwise $\mu_i = +1$ ” “pattern 1”, and that which satisfies “ $\mu_1 = \mu_2 = -1$, otherwise $\mu_i = +1$ ” “pattern 2”. A_1 (resp. A_2) denotes the matrix A with the pattern 1 (resp. pattern 2). The (unnormalized) eigenstates \boldsymbol{v} of A_1 whose eigenvalues have negative imaginary parts are obtained by the following ansatz

$$v_{2n-1} = \alpha^{n-1}, \quad v_{2n} = i\beta\alpha^{n-1} \quad (n = 1, \dots, N/2), \quad (47)$$

where $\alpha, \beta \in \mathbb{C}$ and $|\alpha| < 1$. Letting λ be the eigenvalue of A_1 corresponding to \mathbf{v} , we obtain the following conditions on this ansatz

$$\text{left boundary:} \quad -2i\gamma + 2iJ_x\beta = \lambda_1 \quad (48)$$

$$\text{bulk:} \quad \begin{cases} 2J_x - 2\gamma\beta + 2J_y\alpha = i\beta\lambda_1 \\ 2iJ_y\beta + 2i\gamma\alpha + 2iJ_x\alpha\beta = \alpha\lambda_1 \end{cases}, \quad (49)$$

Here, we neglect the right boundary condition that is justified in the thermodynamic limit. The solution of λ is

$$\lambda_1 = -\frac{i}{2\gamma} \left[-J_y^2 + \sqrt{8\gamma^2(2\gamma^2 + J_y^2 - 2J_x^2) + J_y^4} \right]. \quad (50)$$

In the critical case of $J_x = J_y = 1$, λ has negative imaginary part when $\gamma > 1/\sqrt{2}$, and the gap for pattern 1 (i.e., the argument in parentheses in Eq. (8) for pattern 1) is

$$g_1 = \begin{cases} 2\gamma & (0 \leq \gamma \leq 1/\sqrt{2}) \\ \frac{1}{\gamma} & (1/\sqrt{2} \leq \gamma) \end{cases}. \quad (51)$$

In a similar way, we obtain the localized solution for pattern 2 by the ansatz

$$\begin{cases} v_1 = 1, v_2 = i\delta\beta, \\ v_{2n-1} = \delta\alpha^{n-1}, v_{2n} = i\delta\beta\alpha^{n-1} \quad (n = 2, \dots, N/2) \end{cases}, \quad (52)$$

and conditions

$$\text{left boundary:} \quad \begin{cases} -2i\gamma + 2iJ_x\delta\beta = \lambda_2 \\ 2J_x + 2\gamma\delta\beta + 2J_y\delta\alpha = i\delta\beta\lambda_2 \end{cases} \quad (53)$$

$$\text{bulk:} \quad \begin{cases} 2J_x - 2\gamma\beta + 2J_y\alpha = i\beta\lambda_2 \\ 2iJ_y\beta + 2i\gamma\alpha + 2iJ_x\alpha\beta = \alpha\lambda_2 \end{cases} \quad (54)$$

From these conditions, we obtain in the critical case the gap for pattern 2 as

$$g_2 = \begin{cases} 4\gamma & (0 \leq \gamma \leq \sqrt{(\sqrt{5}-1)/8}) \\ \frac{6^{1/3} \left(9\gamma^2 + \sqrt{48\gamma^6 + 81\gamma^4} \right)^{2/3} - 2 \cdot 6^{2/3}\gamma^2}{3\gamma(9\gamma^2 + \sqrt{48\gamma^6 + 81\gamma^4})^{1/3}} & (\sqrt{(\sqrt{5}-1)/8} \leq \gamma) \end{cases} \quad (55)$$

Finally, we obtain the global gap as

$$\begin{aligned} g &= \min(g_1, g_2) \\ &= \begin{cases} 2\gamma & (0 \leq \gamma \leq \sqrt{(\sqrt{3}-1)/2}) \\ \frac{6^{1/3} \left(9\gamma^2 + \sqrt{48\gamma^6 + 81\gamma^4} \right)^{2/3} - 2 \cdot 6^{2/3}\gamma^2}{3\gamma(9\gamma^2 + \sqrt{48\gamma^6 + 81\gamma^4})^{1/3}} & (\sqrt{(\sqrt{3}-1)/2} \leq \gamma) \end{cases} \end{aligned}$$

Therefore, the transition point γ_c for the critical case is

$$\gamma_c = \sqrt{\frac{\sqrt{3}-1}{2}} \simeq 0.605\dots \quad (56)$$

One may guess that even for topological or trivial case, we can obtain the exact results for the gap in a similar way. However, it would be impossible to obtain the algebraic solutions because in these cases, we need to deal with equations of degree greater than four.

VI. EXACT FORMULA OF THE AUTOCORRELATOR WITH DISSIPATION

The generating function for the weighted Riordan path is obtained as

$$F(z; q, r) := \frac{-1 + (1 - q^2 + r^2)z^2 + \sqrt{[(1 + q^2)z^2 + (1 + rz)^2]^2 - 4q^2z^4}}{2z[q^2rz^2 + (1 + r^2)z + r]}. \quad (57)$$

by the Kernel method. Then, the autocorrelator is recast as

$$C_\infty(t) = \frac{1}{2\pi i} \oint \frac{F(1/w; q, r)}{w} e^{tw} dw \quad (58)$$

$$= \frac{1}{2\pi i} \oint \frac{-w^2 + 1 - q^2 + r^2 + \sqrt{[(w+r)^2 + (1+q)^2][(w+r)^2 + (1-q)^2]}}{2r(w - \eta_+(q, r))(w - \eta_-(q, r))} e^{tw} dw \quad (59)$$

$$\text{where } \eta_\pm(q, r) := \frac{-1 - r^2 \pm \sqrt{(1+r^2)^2 - 4q^2r^2}}{2r}. \quad (60)$$

The contour of w is chosen as shown in Fig. 4, and the final results are

$$C_\infty(t) = \begin{cases} \frac{-\eta_+^2 + 1 - q^2 + r^2}{r(\eta_+ - \eta_-)} e^{\eta_+ t} + \frac{e^{-rt}}{\pi r} \int_{1-q}^{1+q} f(y, q) \frac{(r^{-1} - r)y \cos(yt) + [y^2 - (r + \eta_+)(r + \eta_-)] \sin(yt)}{[y^2 + (r + \eta_+)^2][y^2 + (r + \eta_-)^2]} dy & (0 < q \leq 1) \\ \frac{e^{-rt}}{\pi r} \int_{q-1}^{q+1} f(y, q) \frac{(r^{-1} - r)y \cos(yt) + [y^2 - (r + \eta_+)(r + \eta_-)] \sin(yt)}{[y^2 + (r + \eta_+)^2][y^2 + (r + \eta_-)^2]} dy & (q \geq 1, 0 \leq r < 1) \\ e^{-t} \cos(\sqrt{q^2 - 1}t) + \frac{e^{-t}}{\pi} \int_{q-1}^{q+1} \frac{f(y, q)}{y^2 - q^2 + 1} \sin(yt) dy & (q \geq 1, r = 1) \\ \frac{-\eta_+^2 + 1 - q^2 + r^2}{r(\eta_+ - \eta_-)} e^{\eta_+ t} - \frac{-\eta_-^2 + 1 - q^2 + r^2}{r(\eta_+ - \eta_-)} e^{\eta_- t} + \frac{e^{-rt}}{\pi r} \int_{1-q}^{1+q} f(y, q) \frac{(r^{-1} - r)y \cos(yt) + [y^2 - (r + \eta_+)(r + \eta_-)] \sin(yt)}{[y^2 + (r + \eta_+)^2][y^2 + (r + \eta_-)^2]} dy & (q \geq 1, r > 1) \end{cases}, \quad (61)$$

where

$$f(y, q) = \sqrt{[(q+1)^2 - y^2][y^2 - (q-1)^2]}. \quad (62)$$

In general, it does not have a simpler form. However, in the absence of dissipation, i.e., when $r = 0$, it can be simplified:

$$C_\infty(t; r = 0) = \begin{cases} 1 - q^2 + \frac{1}{\pi} \int_{1-q}^{1+q} \frac{\sqrt{[x^2 - (1-q)^2][(1+q)^2 - x^2]}}{x} \cos(xt) dx & (0 < q \leq 1) \\ \frac{1}{\pi} \int_{q-1}^{q+1} \frac{\sqrt{[x^2 - (q-1)^2][(q+1)^2 - x^2]}}{x} \cos(xt) dx & (q \geq 1). \end{cases} \quad (63)$$

We have confirmed numerically that the integral goes to zero as $t \rightarrow \infty$ in either case. Therefore, the autocorrelator is non-vanishing as $t \rightarrow \infty$ in the topological phase, whereas vanishing in the trivial phase. Moreover, when $q = 1$, it takes a simpler form:

$$C_\infty(t; q = 1, r = 0) = \frac{J_1(2t)}{t}, \quad (64)$$

where J_1 is the Bessel function of the first kind. From the asymptotic behavior of the Bessel function, we obtain that $C_\infty(t)$ decays as $\sim t^{-3/2}$ for large t .

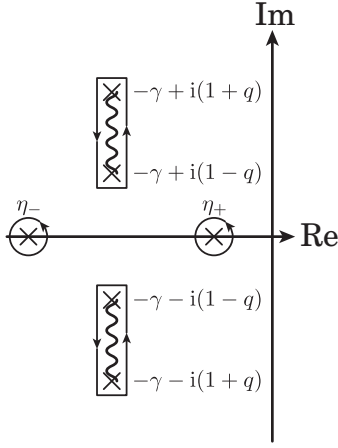
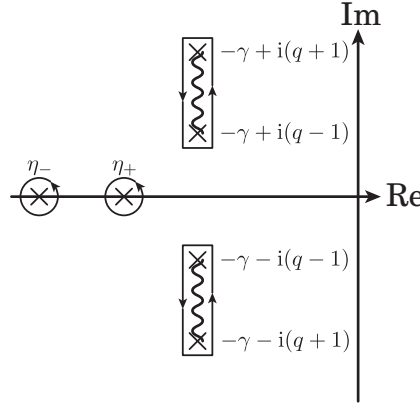
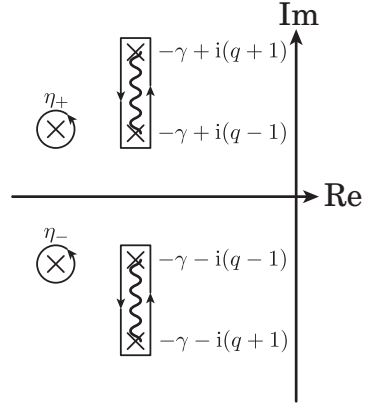
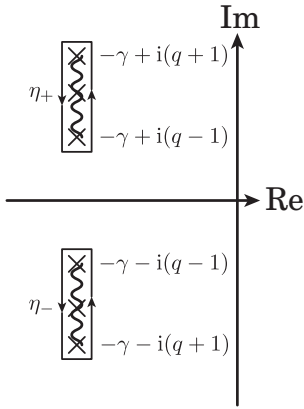
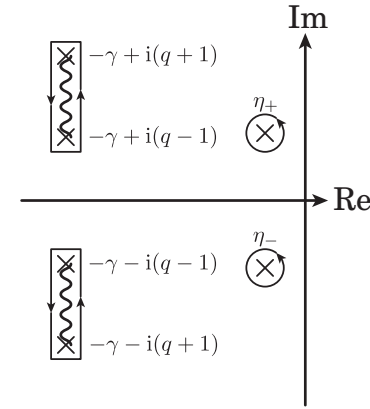
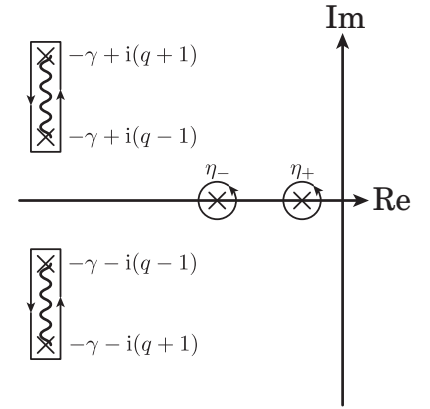
(A) $0 < q < 1$ (B) $q > 1$ (i) $0 < \gamma < q - \sqrt{q^2 - 1}$ (ii) $q - \sqrt{q^2 - 1} < \gamma < 1$ (iii) $\gamma = 1$ (iv) $1 < \gamma < q + \sqrt{q^2 - 1}$ (v) $q + \sqrt{q^2 - 1} < \gamma$ 

FIG. 4. Integration contours of Eq. (60). The crosses (\times) represent poles or branch points, while the wavy lines are branch cuts.